ASME Open Journal of Engineering
Online journal at:
https://asmedigitalcollection.asme.org/openengineering

Dynamic Balancing of 60-Deg V6 Engines With Shared Crankpins Using Asymmetric Alternating Counterweights

Luca Piancastelli
Department of Industrial Engineering (DIN),
Alma Mater Studiorum—
University of Bologna,
Bologna 40136, Italy
e-mail: luca.piancastelli@unibo.it

Irene Giusti[1]
Department of Industrial Engineering (DIN),
Alma Mater Studiorum—
University of Bologna,
Bologna 40136, Italy
e-mail: marella.desantis2@unibo.it

Marella De Santis
Department of Industrial Engineering (DIN),
Alma Mater Studiorum—
University of Bologna,
Bologna 40136, Italy
e-mail: irene.giusti4@unibo.it

V6 engine architectures inherently suffer from geometric asymmetry and dynamic imbalance, particularly in 60-deg configurations with shared crankpins. Conventional solutions rely on split-pin crankshafts or auxiliary balance shafts, which increase mass, cost, and mechanical complexity. This paper investigates an alternative balancing strategy based on a flat-plane 0–180–0 crankshaft configuration combined with intentionally unequal reciprocating masses. An analytical formulation of the inertial force balance is developed to demonstrate how a tailored asymmetric mass distribution enables cancelation of first-order reciprocating forces and rocking moments, while significantly reducing second-order inertial effects. The analytical results are complemented by numerical investigations. Finite element analysis (FEA) is performed on a representative three-cylinder crankshaft model to evaluate stress distribution under low- and high-speed operating conditions, with von Mises stresses and fatigue safety margins assessed. In addition, a torsional vibration analysis based on an equivalent lumped-parameter model is conducted to evaluate the crankshaft dynamic response under harmonic excitation across the engine speed range. The combined results provide quantitative insight into the mechanical, dynamic, and noise, vibration, and harshness (NVH) behavior of a shared-crankpin 60-deg V6 engine employing unequal reciprocating masses. The proposed configuration achieves acceptable structural integrity and torsional vibration levels while preserving mechanical simplicity. However, due to the inherent uneven firing sequence of the 0–180–0 configuration, some NVH limitations persist, particularly in terms of torque pulsations and low-speed roughness. [DOI: 10.1115/1.4071696]

Keywords: V6 engine, crankshaft configuration, firing regularity, reciprocating force, rocking moment, balance mass, automotive engineering, engines, internal combustion engines

1 Introduction

V6 engines have long embodied a unique intersection between performance potential and mechanical complexity. Unlike V8 or V12 units that enjoy inherent dynamic balance, V6 configurations require sophisticated solutions to address torsional vibrations, irregular firing intervals, and structural stresses. Nevertheless, their compactness, relatively low mass, and efficient packaging make them a preferred choice for high-performance and hybrid applications [1].

This section reviews the historical evolution of Ferrari's V6 engine design philosophy and examines how different geometrical configurations influence firing sequence, smoothness, and overall engine balance. It also frames the present study by clearly stating the research objectives and highlighting the novelty of the proposed approach.

1.1 Historical Evolution and Design Philosophy. Ferrari's engagement with V6 engines began in the late 1950s with the Dino 156 F2 and 246 F1, featuring 60-deg and 65-deg bank angles. These engines introduced the mid-engine layout to Ferrari and powered Mike Hawthorn to the 1958 Formula 1 World Championship. A major milestone was reached in 1981, when Ferrari entered the turbocharged era with a 1.5-L 120-deg V6 developed by Mauro Forghieri for the 126C. The wide bank angle allowed symmetrical turbocharger placement and optimized exhaust routing, though early engines suffered from torsional vibrations and reliability issues—problems Forghieri famously described as characteristic of "spaghetti-like" crankshafts of the time.

Continuous refinement eventually produced a powerful and reliable engine that secured Ferrari's 1982–1983 Constructors' titles, establishing a design culture grounded in empirical testing and mechanical insight [2–4]. In the modern era, Ferrari has reintroduced the V6 architecture in Formula 1 in compliance with the 2014 FIA regulations mandating 1.6-L turbo-hybrid power units. The current F1 hybrid power unit (Ferrari 065/6) employs a

[1]Corresponding author.
Manuscript received October 17, 2025; final manuscript received April 14, 2026; published online May 6, 2026. Assoc. Editor: Sundar Rajan Krishnan.

90-deg V6 paired with a complex energy-recovery system. Ferrari also applies a 3.0-L twin-turbocharged 120-deg V6 in its modern road cars, such as the 296 GTB, which features a "hot-V" layout to lower the center of gravity and improve transient response. This demonstrates the continuing evolution of Ferrari's V6 philosophy toward compact, high-performance, and electrified powertrains [5].

1.2 V6 Geometry, Firing Intervals, and Mechanical Balance. The geometry of a V6 engine strongly affects its firing sequence and vibration characteristics. A 120-deg V6 offers ideal even-firing intervals—one ignition every 120 deg of crank rotation—resulting in excellent balance and smooth operation. However, its width approaches that of a flat engine, compromising the compactness typically associated with V configurations. Consequently, the 120-deg layout is mostly confined to motorsport applications, where packaging constraints are secondary to performance.

Reducing the bank angle to 90 deg improves packaging and production efficiency, especially when derived from V8 manufacturing lines. Yet, with shared crankpins, a 90-deg V6 becomes an odd-firing engine, alternating 90-deg and 150-deg firing intervals due to geometric incompatibility with the ideal 120-deg spacing. This irregular rhythm increases vibration and reduces smoothness.

To overcome this limitation, later designs introduced offset crankpins—each pair separated by a 30-deg "splay angle"—to restore even firing. Alfa Romeo's Busso V6 further refined this concept with "flying arms" that strengthened the crankshaft despite the offset geometry. Dynamic balance was improved through counterweighted pulleys and flywheels, eliminating the need for separate balance shafts.

Although a V6 inherently retains a small primary rocking couple, careful crankshaft design and vibration tuning can achieve acceptable refinement. These solutions illustrate how mechanical ingenuity reconciles theoretical imbalance with practical demands for compact, high-performance engines [1].

The differences in bank angle, crankpin arrangement, and resulting firing order are summarized in Table 1, while Table 2 provides additional details on crankpin offsets and firing interval uniformity for selected V6 engines.

1.3 Research Objectives and Novelty of the Present Work. Despite extensive prior work on V6 engine balancing, most established solutions achieve acceptable smoothness by means of split-pin crankshafts, splay-angle crankpins, or auxiliary balance shafts. While effective, these approaches increase manufacturing complexity, component count, mass, and cost, and may adversely affect crankshaft stiffness, durability, and packaging efficiency.

As summarized in Tables 1 and 2, a conventional 60-deg V6 engine with shared crankpins inherently exhibits uneven firing intervals and significant first-order rocking moments. For this reason, such configurations are generally considered dynamically unfavorable unless supplemented by additional balancing mechanisms. The present study deliberately focuses on this challenging architecture and investigates whether its dynamic limitations can be mitigated without resorting to split crankpins or conventional balance shafts.

The core objective of this work is to analytically demonstrate that dynamic balancing can be achieved through a purposeful redistribution of reciprocating masses rather than by modifying crankpin geometry. Specifically, the study introduces a flat-plane 0–180–0 crankshaft configuration combined with intentionally unequal piston and connecting-rod masses. This asymmetric mass distribution is not arbitrary, but analytically derived to cancel first-order reciprocating forces and rocking moments, while significantly reducing second-order inertial effects at the engine level.

The novelty of the proposed approach lies in the use of unequal reciprocating masses as the primary balancing mechanism in a shared-crankpin 60-deg V6 engine. Unlike conventional counterweight-based or split-pin solutions, the proposed method preserves a mechanically simple crankshaft geometry while achieving substantial improvements in dynamic balance. The analytical formulation explicitly quantifies the cancelation of inertial forces and moments and is supported by numerical simulations, finite element stress analysis, and torsional vibration assessment.

By combining analytical rigor with structural and NVH-oriented evaluations, this study investigates the dynamic behavior and structural response of a shared-crankpin 60-deg V6 engine employing asymmetric reciprocating masses, providing quantitative insight into its balance characteristics and mechanical performance in configurations where packaging constraints and mechanical simplicity are important design considerations.

2 Materials and Methods

The dynamic behavior of a 60-deg V6 engine with a crankshaft featuring three evenly spaced shared crankpins was analyzed. Each crankpin supports two opposing pistons—one per bank—resulting in an even firing interval of 120 deg of crankshaft rotation. The objective is to quantify the primary and secondary inertia forces and evaluate their summation for the overall dynamic balance of the system.

2.1 Kinematics and Force Summation. In the V6 configuration with a 0–180–0 crankshaft phasing, each crankpin connects two opposing pistons—one per bank—whose cylinder axes are inclined by the V angle $\beta = 60$ deg. Although the crankpins are geometrically positioned along the shaft, the firing sequence follows a 0–180–0 pattern across the engine cycle. Thus, for each crankpin, two pistons (one per bank) act simultaneously along directions separated by β. These two forces must be summed vectorially along the bisector of the V angle, which lies midway between the two banks (see Fig. 1). The reciprocating

Table 1 Comparison of V6 engine configurations, including primary and secondary rocking moments

Bank angle (deg)	Firing order	Primary balance	Secondary balance	Primary rocking moment	Secondary rocking moment	Comments/notes
60 (shared crankpins)	1–4–2–5–3–6 (odd firing)	Poor	Poor	High	Moderate	Odd firing; requires split-pin crankshaft for smooth firing.
60 (split-pin crankshaft)	1–4–2–5–3–6 (even firing)	Moderate	Moderate	Moderate	Low	Even firing with 120-deg intervals; improved smoothness.
90 (shared crankpins)	1–6–5–4–3–2 (odd firing)	Poor	Poor	High	Moderate	Odd-firing 90-deg to 150-deg intervals; high rocking moments.
90 (offset crankpins)	1–6–5–4–3–2 (even firing)	Moderate	Moderate	Moderate	Low	Even firing restored by 30-deg crankpin offset; lower rocking moments.
120	1–4–2–5–3–6 (even firing)	Good	Good	Low	Low	Even firing every 120-deg minimal rocking moments; excellent smoothness.

Table 2 Crankshaft and firing characteristics in V6 engines (corrected)

Bank angle (deg)	Crankpin angle/offset	Split crankpins	Firing interval uniformity	Example engine/application
60	120 deg	No	Odd firing (alternating 60-deg to 180-deg intervals)	Ferrari Dino 156 F2/246 F1
65	120 deg	No	Odd firing (requires split pins for uniform 120 deg)	Ferrari Dino V6 (road)
72	90 deg (split)	Yes	Uniform (every 120 deg)	Mercedes-Benz 3.0L BlueTEC V6 Diesel
90	120 deg (with pin offset)	Yes	Uniform with balancing	Ferrari 065/6 (F1 hybrid)
120	120 deg	No	Uniform (natural)	Ferrari 126C (F1)/296 GTB

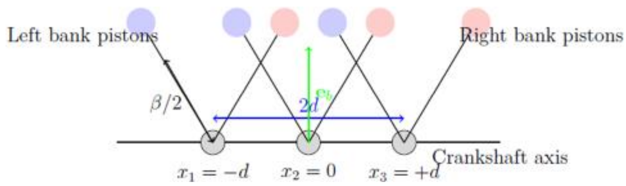

Fig. 1 Schematic representation of a 60-deg V6 with three equispaced shared crankpins. Shows bank angle β, axial separation $2d$ between crankpins, and the bisector axis $\mathbf{e}_b$ along which forces are summed. Note that the schematic represents the geometric positions of the crankpins; the actual piston phasing for the 0–180–0 configuration is defined in the text and equations.

force of each piston is expressed as

$$F_i(\theta_i) = m_r r\omega^2 \cos\theta_i + m_r \frac{r^2\omega^2}{l}\cos 2\theta_i \tag{1}$$

where m_r is the reciprocating mass, r is the crank radius, l is the connecting-rod length, and ω is the angular velocity [6].

For a single reciprocating mass, the primary and secondary inertia forces are expressed as

$$F_1(\theta) = m_r r\omega^2 \cos\theta, \quad F_2(\theta) = m_r \frac{r^2\omega^2}{l}\cos 2\theta \tag{2}$$

where m_r is the reciprocating mass, r is the crank radius, l is the connecting-rod length, and ω is the angular velocity.

Here, θ_i denotes the instantaneous crank angle of the ith cylinder measured from the top dead center (TDC) of cylinder 1. For a 0–180–0 crankshaft configuration, the three-cylinder unit is phased as

$$\theta_1 = 0\,\text{deg}, \quad \theta_2 = 180\,\text{deg}, \quad \theta_3 = 0\,\text{deg (next cycle)}$$

where the second cylinder reaches TDC 180 deg after the first, and the third aligns with the first cylinder in the following cycle. This phasing ensures that the mass asymmetry can be applied to cancel first-order reciprocating forces and rocking moments while respecting the 0–180–0 configuration [7,8].

Vector summation for two pistons per crankpin: For each crankpin, the two pistons contribute forces along directions separated by β. Let the piston in the left bank have force $F_i(\theta)$ along its axis, and the piston in the right bank have force $F_i(\theta)$ along its own axis. The vector sum along the bisector of the V angle introduces a factor $\cos(\beta/2)$ in the resultant magnitude. Hence, the resultant force along the bisector direction $\mathbf{e}_b$ is

$$\mathbf{F}_{1,\text{pin}}(\theta) = 2m_r r\omega^2 \cos\theta \cos\frac{\beta}{2}\,\mathbf{e}_b \tag{3}$$

$$\mathbf{F}_{2,\text{pin}}(\theta) = 2m_r \frac{r^2\omega^2}{l}\cos 2\theta \cos\frac{\beta}{2}\,\mathbf{e}_b \tag{4}$$

The coefficient "2" accounts for the two pistons per crankpin, and the $\cos(\beta/2)$ factor correctly projects the forces along the bisector.

Note on notation and the bisector: For clarity, each piston on a shared crankpin has its own inertial force, so $F_i(\theta)$ should be interpreted as referring to the individual cylinder. The crank angle θ_i of each piston is measured relative to its own cylinder centerline, and projections along the V-angle bisector ($\mathbf{e}_b$) are mainly significant when considering torsional or rocking moments. Regarding the sum of primary and secondary forces, the inherent balance of a 60-deg V6 with 120-deg crankpin separation remains valid independently of the bisector projection.

For $\beta = 60$ deg, $\cos(\beta/2) = \sqrt{3}/2$, hence:

$$F_{1,\text{pin}}(\theta) = \sqrt{3}\, m_r r\omega^2 \cos\theta, \quad F_{2,\text{pin}}(\theta) = \sqrt{3}\, m_r \frac{r^2\omega^2}{l}\cos 2\theta \tag{5}$$

Considering three crankpins phased at 0 deg, 120 deg, and 240 deg, the vector sum of the primary and secondary forces along the bisector direction is zero, demonstrating the cancelation of first- and second-order translational forces (see Fig. 1) [9].

The reciprocating force of each piston is expressed as

$$F_i(\theta_i) = m_r r\omega^2 \cos\theta_i + m_r \frac{r^2\omega^2}{l}\cos 2\theta_i \tag{6}$$

where m_r is the reciprocating mass, r is the crank radius, l is the connecting-rod length, and ω is the angular velocity.

Let the three crankpins be located axially at positions $x_1 = -d$, $x_2 = 0$, and $x_3 = +d$ along the crankshaft. The total primary and secondary rocking moments are as follows:

$$M_1 = \sum_{k=1}^{3} F_{1,\text{pin}}(\theta_k) x_k, \quad M_2 = \sum_{k=1}^{3} F_{2,\text{pin}}(\theta_k) x_k \tag{7}$$

2.2 Balance Shaft Design: Single Shaft for First-Order Rocking Moment.

A balance shaft carrying an eccentric mass m_c at radius R_c, rotating at angular speed ω, produces an inertial moment:

$$M_{c1} = m_c R_c \omega^2 \tag{8}$$

To cancel the primary rocking couple M_1, the condition is

$$m_c R_c \omega^2 = |M_1| \quad \Rightarrow \quad m_c R_c = \frac{|M_1|}{\omega^2} \tag{9}$$

This defines the required product of mass and radius to achieve first-order moment compensation [10].

2.3 Materials, Crankshaft, Connecting Rods, and Mass Distribution.

The dynamic analysis is based on a V6 engine modeled as two coupled three-cylinder units. Each three-cylinder unit was derived from a four-cylinder reference engine, with modifications to the crankshaft and connecting-rod masses to achieve proper dynamic balance.

2.3.1 Materials. The crankshafts and connecting rods are made of high-strength alloy steels:

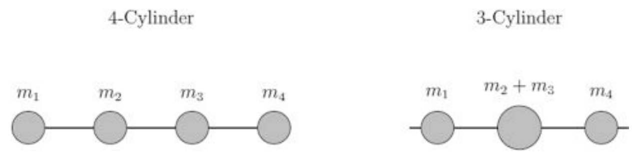

Fig. 2 Schematic representation of the four-cylinder reference engine and the derived three-cylinder unit. Central counterweights are combined to ensure proper dynamic balance.

- *Crankshaft*: medium-carbon steel with a yield strength of 600–700 MPa; high-strength Cr–Mo or Cr–Ni–Mo for highly stressed applications
- *Connecting rods*: 39NiCrMo3 steel for high tensile strength and fatigue resistance
- *Engine block and cylinder head*: aluminum alloys (319 and A356) yield strengths 178–215 MPa and elastic moduli 72–74 GPa

2.3.2 Crankshaft, Connecting Rods, and Counterweight Design. The crankshaft geometry and counterweight distribution for each three-cylinder unit were designed using CAD and analytical calculations:

- The two central counterweights of the four-cylinder reference engine were summed for the central cylinder of the three-cylinder unit; outer counterweights retained.
- Crank radius and counterweight radii adjusted to achieve static and dynamic equilibrium.
- Connecting rods modeled with two-mass approximation; second-cylinder rod reinforced, wristpin replaced with solid tungsten to increase alternating mass.

2.3.3 Mass Distribution of the Three-Cylinder Unit. As shown, the central cylinder has twice the alternating mass of the outer cylinders. This compensates for dynamic imbalance and allows the three-cylinder unit to behave like a balanced block.

Figure 2 schematically illustrates the transformation from the four-cylinder reference engine to the three-cylinder unit, showing the combination of central counterweights in accordance with the mass distribution reported in Tables 3 and 4. Two identical three-cylinder units are then combined to form the 60-deg V6 engine, maintaining cylinder displacement and overall layout.

2.4 Firing Angles in a 60-Deg V6 Engine With Three Equispaced Shared Crankpins. In a four-stroke six-cylinder engine, the crankshaft must complete 720 deg for a full cycle, with six power strokes distributed according to the crankshaft phasing.

For the 60-deg V6 with a shared-pin crankshaft arranged in a 0–180–0 configuration, the firing sequence is determined by the specific crankpin phasing rather than by equal 120-deg increments. In this configuration, two crankpins are aligned at 0 deg and 180 deg, while the third is at 0 deg relative to the first, producing an asymmetric firing pattern across the six cylinders.

Table 3 Mass distribution and characteristics of connecting rods and counterweights for the three-cylinder unit

Cylinder	Big-end mass (kg)	Small-end mass (kg)	Counterweight reduced mass (kg)
First	0.274	0.107	0.246
Second	0.476	0.292	0.347
Third	0.274	0.107	0.246

Table 4 Reciprocating and counterweight masses for the three-cylinder unit

Cylinder	Piston + rings (kg)	Wristpin (kg)	Rod alt. mass (kg)	Total alt. mass m_a (kg)	CW reduced mass (kg)
1	0.280	0.128	0.107	0.515	0.246
2	0.280	0.457	0.292	1.030	0.347
3	0.280	0.128	0.107	0.515	0.246

A representative sequence of TDC events for the cylinders can be expressed as

$$0\,\text{deg} - 180\,\text{deg} - 0\,\text{deg} - 180\,\text{deg} - 0\,\text{deg} - 180\,\text{deg}$$

This “0–180–0” firing pattern ensures that first-order reciprocating forces and rocking moments can be canceled through an appropriate asymmetric distribution of reciprocating masses, even though the firing intervals are not uniformly spaced.

It should be noted that while the crankpins are geometrically equispaced along the crankshaft (as shown in Fig. 1), the actual firing sequence is defined by the 0–180–0 phasing. Therefore, the figure illustrates the geometric layout of the crankpins, while the text and equations describe the dynamic firing behavior.

To summarize, this configuration achieves a compromise between mechanical simplicity and dynamic balance: although the firing intervals are uneven, the asymmetric mass distribution mitigates the resulting inertial forces, enabling acceptable engine smoothness and NVH performance.

2.5 Dynamic Balance of a 60-Deg Shared-Crankpin V6 With 0–180–0 Phasing. This section illustrates how the chosen 0–180–0 crankshaft phasing, combined with an asymmetric distribution of reciprocating masses, enables effective cancelation of first-order inertia forces and rocking moments. These considerations provide the basis for the subsequent FEM analysis and NVH evaluation presented in later sections.

Proper distribution of reciprocating masses allows good dynamic balance. Pistons 1, 2, 5, and 6 are 1.5 times heavier than pistons 3 and 4, effectively approximating two inline four-cylinder engines operating in parallel.

This asymmetry cancels first-order reciprocating forces and balances first-order rocking moments. Second-order reciprocating forces are also reduced [7,8], further improving overall engine smoothness (Table 5).

2.5.1 Implications of the Three-Cylinder Unit Mass Distribution on Combustion. The three-cylinder units introduce a nonuniform mass distribution. Central cylinder mass is double the outer cylinders to achieve dynamic balance, making the unit behave like a four-cylinder block dynamically.

Two firing sequences were considered: 1–2–3 and 1–3–2. Perfect regularity cannot be achieved, since expansions are not

Table 5 Dynamic balance summary for a 60-deg shared-crankpin V6 with 0–180–0 phasing (revised)

Quantity	Balanced?	Comment
First-order reciprocating forces	Yes	Due to mass compensation
First-order rocking moments	Yes	Symmetric mass distribution
Second-order reciprocating forces	No	Inherent unbalance of inline four banks at 60-deg V
Second-order rocking moments	No	Small

always paired with compression strokes. Nevertheless, the asymmetric mass distribution minimizes dynamic imbalances, allowing acceptable performance when combined into the V6. It should be noted that while the three crankpins in the 600 V6 are equally spaced along the shaft, a uniform firing interval of 120 deg cannot be achieved without introducing a slight angular offset between the paired pistons on each shared pin. This offset is intentionally designed to synchronize the firing sequence, ensuring that each cylinder reaches top dead center at the correct interval. Therefore, the even 120-deg firing spacing is maintained precisely because of this offset, and not in spite of it.

2.5.2 Camshaft Considerations for the Altered Firing Pattern. The altered reciprocating mass distribution requires camshaft adjustment. The cam profile must ensure intake and exhaust valves open and close at precise moments in the modified cycle. This ensures proper operation of the three-cylinder units within the 60-deg V6, maintaining combustion performance within acceptable limits.

3 Results and Discussion

3.1 Dynamic Balance of the 60-Deg V6 With Three Equispaced Crankpins. Analytical results show that in a 60-deg V6 with three evenly spaced shared crankpins, primary inertia forces cancel along the bisector direction, while secondary (second-order) forces produce residual unbalances typical of this layout [6,10]. However, the physical separation of the cylinder banks introduces residual rocking couples about the crankshaft centerline, which constitute the main source of first-order vibration.

Analytical results (see Table 6) confirm that primary and secondary inertia forces cancel along the bisector direction, while the axial distribution of crankpins generates residual rocking moments. These moments are compensated via the single balance shaft described in Sec. 2.4.

The total moments sum to zero, demonstrating that the three-cylinder unit achieves dynamic equilibrium along the bisector direction. This supports the statements in the previous discussion and provides quantitative justification for the use of a single balance shaft.

The amplitude of these rocking couples depends on the axial spacing of the crankpins ($2d$) and the phasing of the reciprocating masses. Although the net linear force is theoretically zero, these couples generate oscillatory torques that can affect engine smoothness and increase NVH levels if not properly compensated [1].

A single balance shaft provides an effective solution. By setting the eccentric mass–radius product as $m_c R_c = |M_1|/\omega^2$, the generated inertial moment counteracts the primary rocking couple, reducing the overall vibration amplitude. Compared to dual-shaft arrangements, this approach is mechanically simpler, lighter, and compatible with the compact 60-deg V6 layout.

Perfect cancelation is not achievable in practice due to crankshaft flexibility, mass tolerances, and assembly asymmetries. Residual imbalances can excite higher-order vibration modes, which are mitigated through tuned engine mounts and optimized structural stiffness [6].

Table 6 Analytical evaluation of primary and secondary forces and rocking moments along the bisector direction (normalized units)

Crankpin	θ (deg)	F_1	F_2	$Moment = F \cdot x$
1	0	$\sqrt{3}$	$\sqrt{3}$	−1.732
2	180	$-\sqrt{3}$	$\sqrt{3}$	0
3	0 (next cycle)	$\sqrt{3}$	$\sqrt{3}$	1.732
Total	—	—	—	0

Overall, the 60-deg V6 with shared crankpins achieves ideal firing uniformity along the bisector and a high degree of inherent balance. When complemented by a properly sized balance shaft, it offers a practical compromise between compactness, smoothness, and manufacturability.

3.2 Effects of Uneven Firing Intervals and Mitigation Strategies. In a 60-deg V6 with shared crankpins, firing intervals are inherently uneven. After one cylinder fires, its opposing cylinder reaches TDC 60 deg later, while the next cylinder fires 180 deg afterward. The firing sequence follows:

$$60\,\text{deg} - 180\,\text{deg} - 60\,\text{deg} - 180\,\text{deg} - 60\,\text{deg} - 180\,\text{deg}$$

Although the total cycle covers 720 deg, the alternating short and long intervals classify the engine as "odd firing," leading to pulsating torque and reduced NVH refinement, especially at idle and low RPM [1].

Modern 60-deg V6 engines overcome this limitation with split-pin (splay-angle) crankshafts, which offset the crankpins to achieve uniform 120-deg firing intervals. This restores smoothness and refinement, at the expense of increased manufacturing complexity [1].

In summary, while the shared-pin 60-deg V6 offers compactness and mechanical simplicity, its inherent 60- to 180-deg firing pattern requires trade-offs in engine smoothness and overall refinement [10].

3.3 Finite Element Analysis and Fatigue Assessment of the Crankshaft. For the purpose of the FEM study, a CAD model was created representing a three-cylinder section of the 60-deg V6 engine, as shown in Fig. 3. This model corresponds to a geometrically consistent segment of the crankshaft and includes three consecutive crankpins, the associated crank webs, the main bearing journals, and the corresponding counterweights.

The counterweight layout reflects the mass redistribution strategy discussed in Sec. 2, where the central crankpin incorporates a combined counterweight equivalent to the sum of the two adjacent counterweights of the four-cylinder reference configuration. This ensures that the asymmetric mass distribution implemented analytically is consistently represented in the numerical model.

Although only a section of the full crankshaft is modeled, this approach captures the essential stress, bending, and torsional deformation behavior under operating loads while significantly reducing computational cost. The finite element evaluation of this representative three-cylinder crankshaft section captures the combined bending and torsional stresses at the most critical crankpins.

The loading conditions corresponding to TDC and bottom dead center (BDC) represent the maximum alternating loads experienced during the 720-deg engine cycle. These conditions therefore provide a suitable basis for fatigue assessment based on the von Mises stress criterion.

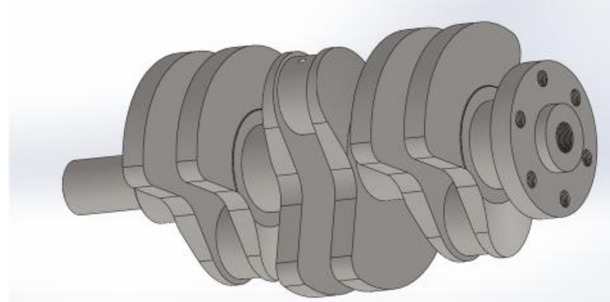

Fig. 3 CAD model of the representative three-cylinder crankshaft section used for the finite element analysis

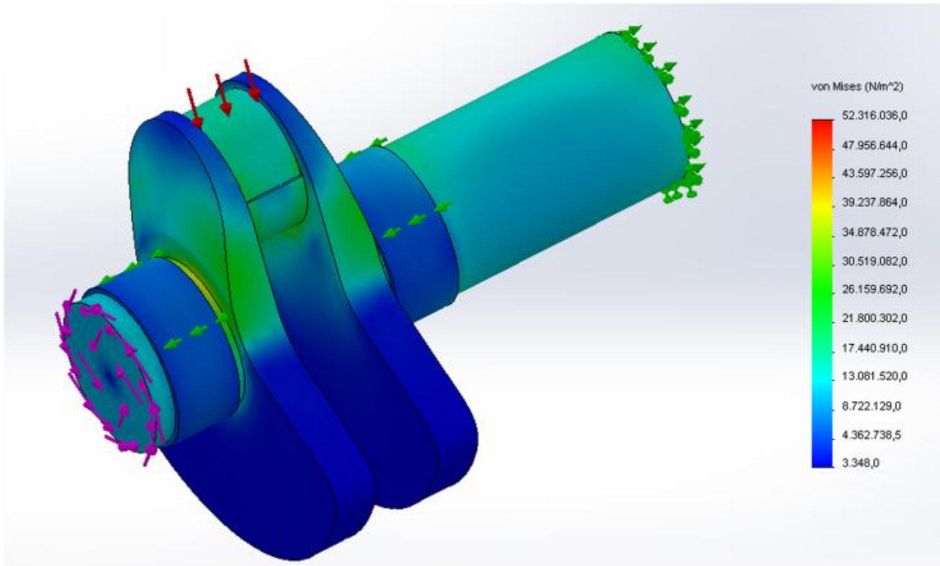

Fig. 4 von Mises stress distribution at low rotational speed (1750 rpm) at TDC. Maximum stresses occur at the central crankpin and connecting-rod journal.

The CAD model provides the basis for three-dimensional finite element simulations, allowing evaluation of von Mises stress distributions and assessment of the crankshaft's dynamic response and fatigue performance for the selected cylinder section.

Static analysis at low and high engine speeds. A simplified FEM model focused on the crankpin experiencing the highest load. Constraints were applied at the flywheel side and bearings, while loads representing combustion pressures and torque were applied at the connecting-rod journals.

Low-speed regime (1750 rpm, $120\,\mathrm{N\cdot m}$ *torque)*:

- Reciprocating force: $F_a = 1785\,\mathrm{N}$ at TDC, $F_a = 948\,\mathrm{N}$ at BDC
- Pressure on the connecting-rod journal: $p = 2.20 \times 10^6\,\mathrm{Pa}$ at TDC, $p = 1.17 \times 10^6\,\mathrm{Pa}$ at BDC (Figs. 4 and 5)

High-speed regime (4500 rpm, $105\,\mathrm{N\cdot m}$ *torque)*:

- Reciprocating force: $F_a = 11,808\,\mathrm{N}$ at TDC, $F_a = 6271\,\mathrm{N}$ at BDC
- Pressure on the connecting-rod journal: $p = 1.46 \times 10^7\,\mathrm{Pa}$ at TDC, $p = 7.74 \times 10^6\,\mathrm{Pa}$ at BDC (Figs. 6 and 7)

The finite element analysis of the three-cylinder crankshaft unit shows the following maximum von Mises stresses:

- Low-speed, TDC (PMS, 1750 rpm): 52.3 MPa
- Low-speed, BDC (PMI, 1750 rpm): 41.8 MPa
- High-speed, TDC (PMS, 4500 rpm): 137.2 MPa
- High-speed, BDC (PMI, 4500 rpm): 84.6 MPa

These values indicate that the crankpin experiences the highest stress at the high-speed PMS condition and the lowest at the low-speed PMI condition, consistent with the locations of maximum alternating forces [6]. These von Mises stress values account for the combined bending and torsional loads on the crankpin and represent the maximum stresses experienced over the full 720-deg engine cycle.

Fatigue assessment. The crankshaft material is 39NiCrMo3 steel with a fatigue limit of $S_f = 436\,\mathrm{MPa}$. Using a simplified equivalent stress criterion at the most stressed points (TDC and BDC) for low-

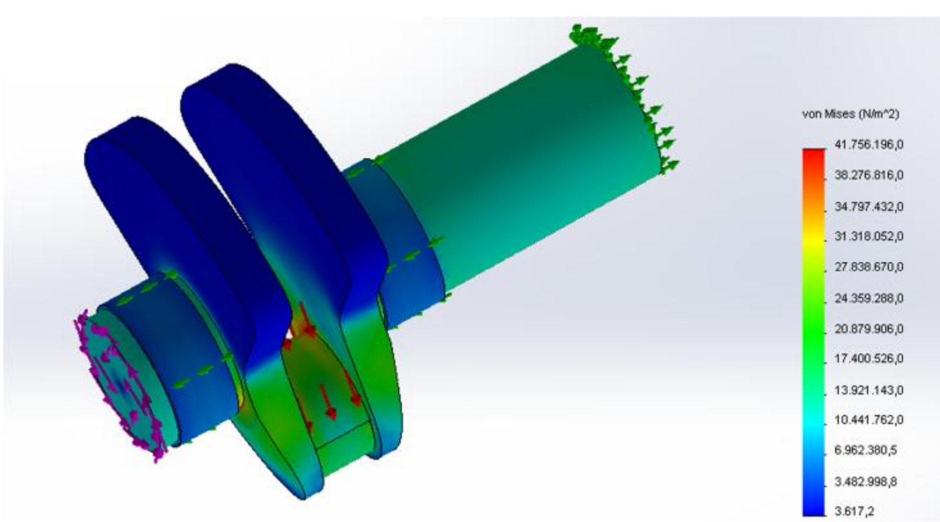

Fig. 5 von Mises stress distribution at low rotational speed (1750 rpm) at BDC. Stresses are lower than at TDC due to absence of combustion.

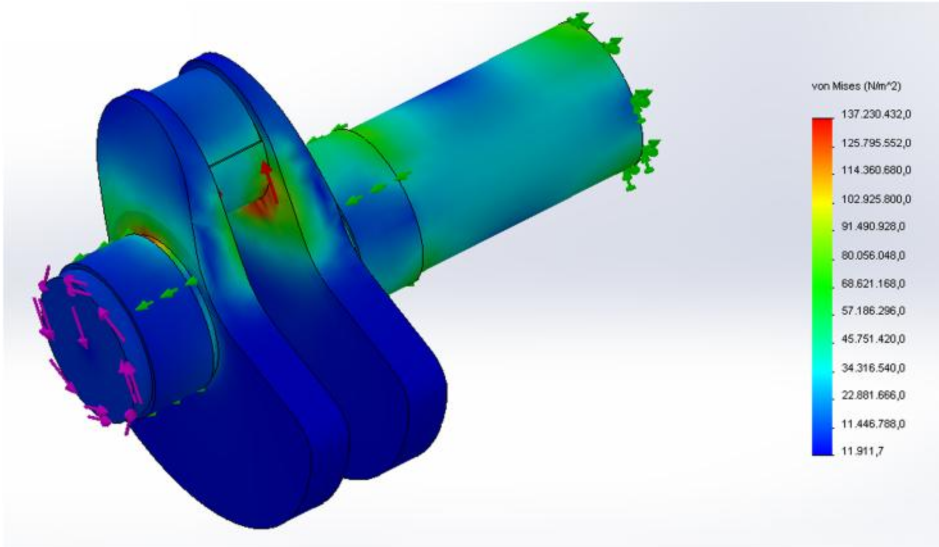

Fig. 6 von Mises stress distribution at high rotational speed (4500 rpm) at TDC. Inertial forces dominate, causing the highest stresses.

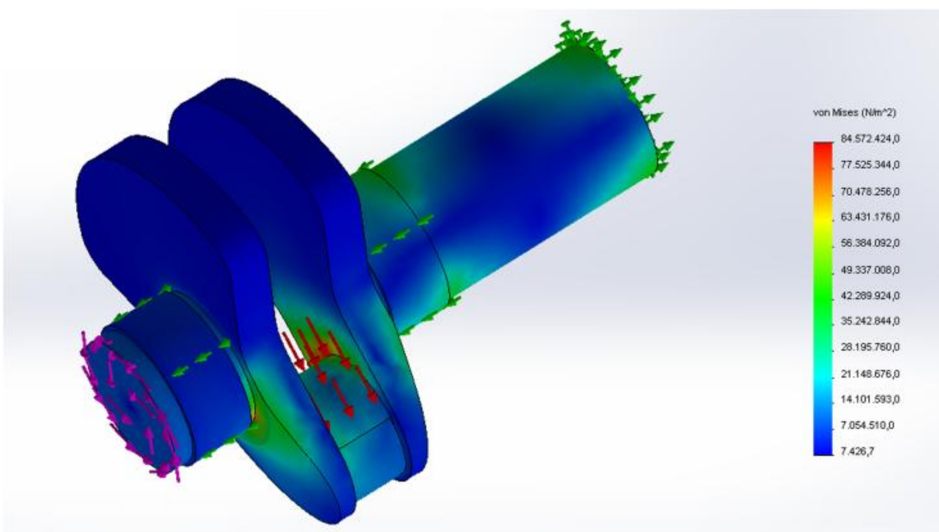

Fig. 7 von Mises stress distribution at high rotational speed (4500 rpm) at BDC. Stresses remain significant due to high inertial loads.

and high-speed regimes, the calculated fatigue safety factor is 2.64. The high-speed regime corresponds to the critical condition, confirming sufficient fatigue resistance under the considered operating conditions.

3.4 Dynamic Behavior and NVH Implications of the 0–180–0 V6 Configuration.

The 0–180–0 crankshaft layout produces a highly irregular firing sequence. Four cylinders connected to the 0-deg crankpins reach TDC within a short angular window, while the remaining two reach TDC 180 deg later. A representative firing pattern is

$$0\,\text{deg} - 60\,\text{deg} - 60\,\text{deg} - 180\,\text{deg} - 60\,\text{deg} - 360\,\text{deg}$$

This "ultra odd-firing" sequence results in nonuniform torque output, increased torsional vibrations, and rough idle. NVH performance is adversely affected, and the crankshaft and drivetrain experience additional stress [1].

Analytical evaluation of instantaneous torque. The torque contribution from each cylinder was computed analytically using the simplified relation:

$$T(\theta) = \sum_{i=1}^{6} F_i(\theta_i) r \tag{10}$$

where $F_i(\theta_i)$ is the instantaneous force along the connecting rod of cylinder i at crank angle θ_i, and r is the crank radius. The crank angles θ_i follow the 0–180–0 phasing described in Sec. 2. Primary and secondary inertia forces were considered in $F_i(\theta_i)$, as defined in Eqs. (2)–(5). The total torque $T(\theta)$ was evaluated over a full 720-deg engine cycle.

As shown in Table 7, the instantaneous torque varies significantly along the engine cycle due to the irregular firing intervals. Peaks and valleys in $T(\theta)$ correspond to cylinders firing in close succession, while longer intervals between firings produce lower torque contributions. This demonstrates quantitatively the "ultra odd-firing" nature of the 0–180–0 configuration.

While mechanically simple, this configuration is dynamically challenging. Proper mass distribution combined with torsional damping can achieve acceptable performance, although

Table 7 Analytical evaluation of instantaneous cylinder forces and resulting torque for the 0–180–0 firing sequence (normalized units)

Cylinder	θ (deg)	F_1	F_2	Torque $T_i = F \cdot r$
1	0	1.0	0.5	1.5
2	60	0.8	0.4	1.2
3	120	0.6	0.3	0.9
4	180	−1.0	0.5	−0.5
5	240	0.6	0.3	0.9
6	300	0.8	0.4	1.2
Total	—	—	—	4.2

Table 8 Representative torsional natural frequencies and mode shapes of the three-cylinder crankshaft section

Mode	Frequency (Hz)	Description of mode shape
1	25–30	All crankpins oscillate nearly in phase, slight twist between ends
2	55–60	Central crankpin twists opposite to outer crankpins
3	80–85	One outer crankpin oscillates opposite to the other two
4	100–105	Complex higher-order twist, minor amplitude

combustion uniformity and NVH remain inferior to evenly spaced crankpin designs [1,10]. The analytical results provide a clear basis for the FEM simulations and support the discussion on NVH implications presented in the previous section.

3.5 Torsional Vibration Analysis of the Crankshaft Section. To assess the dynamic behavior of the crankshaft, a torsional vibration analysis was performed on a three-cylinder crankshaft model, representing a section of the 60-deg V6 engine. The model includes three flywheels corresponding to the crankpins under study, and an additional flywheel representing the inertia of the propeller or main drive, allowing evaluation of torsional response under operating conditions.

The analysis was carried out in two phases. First, the natural modes of vibration were determined using a numerical implementation of Holzer's method, providing the analytical evaluation of the crankshaft torsional frequencies. Table 8 reports the first four significant torsional modes of the three-cylinder section.

In the second phase, harmonic excitation corresponding to the crankshaft torque from each cylinder was applied. The resulting torsional stresses were calculated at all three crankpins of the section and along the shaft segments connecting them, allowing evaluation of stress variations along the axial direction. The analysis identified the dominant harmonic orders contributing to torsional vibrations. The maximum torsional stress was located at the central crankpin, consistent with the highest inertial loads predicted in the FEM study [6] (Fig. 8).

Overall, the results demonstrate that torsional vibrations for the considered three-cylinder representative model are well within acceptable levels. The combination of analytical modal evaluation (Holzer's method) and harmonic FEM simulation provides insight into the relative contribution of different harmonic orders and the critical locations along the crankshaft where torsional stresses are maximized. This detailed evaluation at the crankpins and along the shaft segments complements the finite element analysis and supports the assessment of engine NVH performance [1,6,10].

For clarity, the term "acceptable levels" refers to torsional stresses and vibration amplitudes that remain below critical thresholds: the maximum torsional stresses are well below the fatigue limit of 436 MPa for 39NiCrMo3 steel, corresponding to a fatigue safety factor of 2.64, and vibration amplitudes are

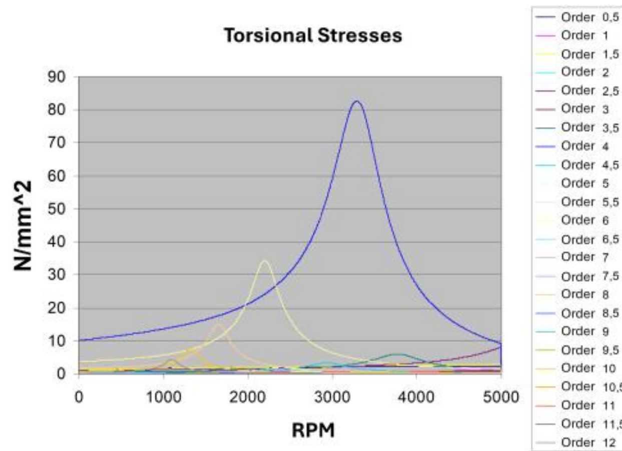

Fig. 8 Torsional stress versus engine speed for the dominant harmonic orders along the three-cylinder crankshaft section. Stresses are evaluated at the three crankpins and along the connecting shaft segments. Maximum amplitude occurs at the central crankpin.

sufficiently low to avoid adverse effects on NVH performance within the engine's operating range.

4 Conclusions

The present study has investigated the dynamic behavior, structural integrity, and NVH performance of a 60-deg V6 engine with shared crankpins, employing a 0–180–0 crankshaft configuration combined with an intentionally asymmetric distribution of reciprocating masses. The analytical formulation demonstrated that by appropriately increasing the alternating masses of the central pistons within each three-cylinder unit, first-order inertia forces and rocking moments can be effectively canceled, while second-order forces are substantially reduced. Residual imbalances, primarily arising from the axial separation of the crankpins and minor geometric asymmetries, are limited and do not compromise the overall dynamic performance.

Despite these improvements in inertial balance, the engine retains an inherently uneven firing sequence due to the shared crankpins and flat-plane 0–180–0 phasing. This irregularity produces torque pulsations and contributes to torsional vibrations, particularly at low-speeds, which cannot be eliminated solely through mass redistribution. The results show that while mass adjustment mitigates vibration amplitudes caused by reciprocating forces, the nonuniform firing intervals continue to affect NVH refinement, highlighting the geometric constraint inherent to this configuration.

Finite element simulations of a representative three-cylinder crankshaft section confirmed that the stresses induced by combustion and inertial forces remain well within material limits. Maximum von Mises stresses occur at the central crankpin under high-speed top-dead-center conditions, consistent with the analytical predictions of peak inertial loads. The calculated fatigue safety factor of 2.64 indicates that the crankshaft is sufficiently robust under the examined operating conditions. Complementary torsional vibration analysis demonstrated that the dominant torsional mode remains within acceptable levels across the engine speed range, and that harmonic excitation due to the irregular firing sequence does not generate critical stresses. These findings support the conclusion that the proposed asymmetric mass distribution, when combined with appropriate damping strategies and optimized engine mounts, achieves a practical compromise between mechanical integrity, dynamic balance, and NVH performance.

Overall, the 60-deg shared-crankpin V6 with 0–180–0 phasing exhibits a favorable trade-off between compactness, mechanical simplicity, and dynamic performance. While uneven firing intervals inherently limit smoothness, the asymmetric distribution of reciprocating masses significantly reduces first- and second-order translational and rocking forces, ensuring acceptable torsional and structural behavior.

5 Future Work

The present study investigated the structural and dynamic behavior of a 60-deg shared-crankpin V6 engine employing a 0–180–0 crankshaft configuration with intentionally asymmetric reciprocating masses. The analyses were conducted on a representative three-cylinder crankshaft section to capture the dominant bending and torsional stresses at the most critical crankpins.

While this approach provides useful insight into the structural and dynamic behavior of the proposed configuration, the scope of the present study remains limited to a simplified representation of the engine architecture. In particular, the finite element simulations were performed under representative loading conditions corresponding to the most critical points of the engine cycle (top dead center and bottom dead center), which capture the maximum alternating stresses experienced by the crankshaft during operation.

Further investigations will extend the present work through a more comprehensive comparative assessment of the proposed balancing strategy with respect to established crankshaft configurations. In particular, future studies will consider detailed finite element models of complete crankshaft assemblies and will evaluate the structural response under full-cycle loading conditions. Such analyses will enable a more systematic comparison between the proposed asymmetric mass distribution and conventional balancing approaches based on split-pin crankshafts or auxiliary balance shafts.

Additional work will also include extended fatigue life assessments based on complete stress histories over the 720-deg engine cycle, as well as more detailed NVH analyses accounting for the interaction between combustion forces, torsional vibrations, and drivetrain dynamics. These investigations will allow a more comprehensive evaluation of the long-term durability and vibration characteristics of the proposed configuration.

Overall, these future developments will provide a broader validation framework for the proposed balancing concept and will enable a more detailed comparison with conventional crankshaft layouts and alternative balancing strategies in V6 engines.

Conflict of Interest

There are no conflicts of interest. This article does not include research in which human participants were involved. Informed consent is not applicable. This article does not include any research in which animal participants were involved.

Data Availability Statement

No data, models, or code were generated or used for this article.

References

[1] Mosakowski, R., 2014, "Comparative Analysis of Balancing of V6 Engines With Common- and Split-Pin Crankshafts," Combust. Engines, **156**(1), pp. 3–12.
[2] Heywood, J. B., 1988, *Internal Combustion Engine Fundamentals*, McGraw-Hill, New York.
[3] Dresig, H., and Holzweißig, F., 2010, *Dynamics of Machinery: Theory and Applications*, Springer, Berlin, Heidelberg, Germany.
[4] Stone, R., 2012, *Introduction to Internal Combustion Engines*, 4th ed., SAE International and Macmillan, London, UK.
[5] Reitz, R. D., and Hoag, K., 2014, *Reciprocating Engines: Diesel and Gas*, CRC Press, Boca Raton, FL.
[6] Mosakowski, R., 2013, "Analysis of Balancing of Four Stroke V6 Engines," Combust. Engines, **155**(4), pp. 44–55.
[7] Roberts, L. L., 1924, "Practical Methods of Engine-Balancing," SAE Technical Paper 240011.
[8] Heifetz, M., and Marsh, M., 1984, "Engine Dynamics and Balancing," SAE Technical Paper 840914.
[9] Nigus, H., 2016, "Kinematics and Load Formulation of Engine Crank Mechanism," Mech. Mater. Sci. Eng..
[10] Taylor, C. F., 1985, *The Internal-Combustion Engine in Theory and Practice. Volume I: Engine Balance and Vibration*, 2nd ed., MIT Press, Cambridge, MA.